PARTIAL TORQUE RIDE THROUGH WITH MODEL PREDICTIVE CONTROL

Paper No. PCIC Europe BER-42

Thomas Besselmann
ABB Corporate Research
Segelhofstr. 1k
5405 Baden-Dättwil
Switzerland

Pieder Jörg
ABB MV Drives
Austrasse
5300 Turgi
Switzerland

Terje Knutsen
Statoil Res. & Technol.
Martin Linges vei 33
1364 Fornebu
Norway

Erling Lunde
Statoil Res. & Technol.
Arkitekt Ebbells veg 10
7005 Trondheim
Norway

Tor Olav Stava
Gassco AS
Bygnesvegen 75
4250 Kopernik
Norway

Sture Van de moortel
ABB MV Drives
Austrasse
5300 Turgi
Switzerland

Abstract - Symmetric and asymmetric dips of the grid voltage pose serious problems to gas compression stations powered by drives such as load commutated inverters (LCI). Drive control systems used in industrial practice are not capable to handle reduced grid voltage situations appropriately, and execute a ride-through procedure instead during which no drive torque is provided by the drive. Without drive torque compressors may quickly enter surge conditions, under which the gas flows rapidly back and forth, causing wear and risking damage to the equipment. In this paper we describe a novel control approach developed for load commutated inverters based on model predictive control (MPC). Model predictive control is an optimization-based control method, where a mathematical model of the system is used to determine control inputs which are optimal with respect to some objective function. With the revised control system, the drive is capable to provide partial drive torque during grid disturbances; thus resulting in robustness improvements for electrically-driven gas compression stations. In the case of a voltage dip, the compressor is still supplied with partial drive torque, decreasing the probability of the compressor diverging into surge. The paper includes experimental results executed on two real 41.2 MW LCI-fed synchronous machines each powering a gas compressor.

Index Terms — Gas compressors, variable speed drive, load commutated inverter, model predictive control.

I. INTRODUCTION

Electrically-driven gas compressors have a number of advantages compared to compressors driven by gas turbines: (a) the drive torque can be varied much quicker, (b) the variable-speed drive system can be operated with high efficiency in a much broader operation range and (c) there are no local greenhouse gas emissions. In situations such as subsea installations a variable speed drive (VSD) system may be the only option to power gas compressors [1], [2]. Due to the aforementioned reasons, a number of large gas processing plants in Norway employ electrically-driven gas compressors.

Gas compression is energy-intensive, such that high power solutions for the variable speed drive are sought. A typical solution consists of a synchronous machine fed by a load commutated inverter (LCI). Reasons for this choice are the proven reliability of the LCI combined with its competitive price in high power applications [3].

One of the gas compression sites is the basis for the technical innovation described in the paper. This gas treatment plant is located at a remote location and is affected by disturbances in the Norwegian electricity grid. Weather phenomena such as storms occasionally cause brief impairments of the power lines, resulting in a sudden reduction of the grid voltage in one or more phases. Typically the grid voltage is affected over a time span of 50 to 150 ms.

While of short duration, the consequences of these voltage dips can be severe. They can cause the LCI to trip, e.g. due to inrush currents at the return of the grid voltage. Or, due to the sudden loss of drive torque, the compressor may enter unstable operating conditions such as surge or rotating stall, and is tripped as a precaution to avoid mechanical damage and wear. In either case the operation of the gas compressor, and after a short time the upstream plant, is stopped and a time-consuming restarting procedure needs to be carried out. Since the amount of exported gas is considerable, the financial cost of such an incident can be immense.

The paper describes a novel torque control scheme and its commissioning on load commutated inverters powering two 41.2 MW gas compressors. The goal of this new control scheme is to increase the robustness of the torque controller in the case of grid disturbances. In particular partial torque shall be provided during partial loss of grid voltage. The proposed control scheme is based on model predictive control (MPC), an optimization-based control method [4], and requires the solution of a mathematical optimization problem at each millisecond on an embedded system [5].

The paper is structured as follows: After this introduction, preliminaries are summarized in Section II. Section III states technical information about the gas processing plant of interest. The proposed MPC solution is outlined in Section IV. The verification of the control solution during grid disturbances is shown on a Hardware-in-the-Loop (HIL) simulator, Section V. Subsequently measurements from the commissioning of the novel control algorithm on site and from a real voltage dip event are reported in Sections VI and VII, respectively. A list of abbreviations can be found in Table 1.

TABLE 1
LIST OF ABBREVIATIONS

Abbreviation	Meaning
AC	alternating current
DC	direct current
FPGA	field programmable gate array
HIL	hardware in the loop
I/O	input / output
LCI	load commutated inverter
MPC	model predictive control
MV	medium voltage
QP	quadratic program
SQP	sequential quadratic program
VSD	variable speed drive

II. PRELIMINARIES

In this section we take a closer look on grid disturbances. Depending on the reaction of the frequency converter, different types of ride through behaviour are distinguished. More information is provided in [6].

A. Symmetric Vs. Asymmetric Voltage Dips

In an ideal three-phase system, the voltages in the three phases are sinusoidal with the same amplitude, succeeding each other with a phase shift of 120 degree. By means of the alpha-beta transformation (also known as Clarke transformation), the three phase voltages can be mapped into the two-dimensional plane, where the ideal voltages correspond to a voltage vector rotating on a circle, [7].

In the case of *symmetric* grid disturbances the amplitude of all three phases is reduced by the same amount, whereas the phase difference is unaffected. In the alpha-beta plane this corresponds to circles with varying radii. Figure 1 shows a practical example of a symmetric voltage dip, as measured on the primary side of the transformer at a large gas processing plant in Norway.

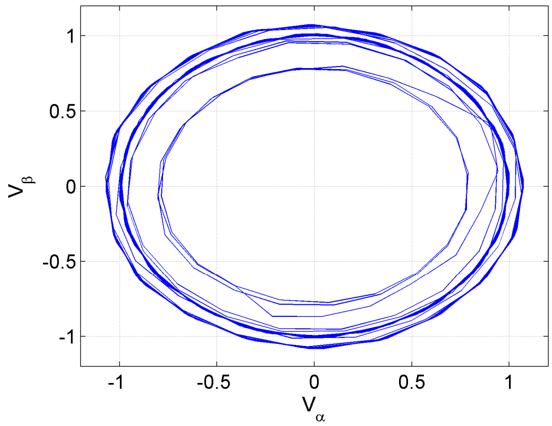

Fig. 1: Example for symmetric grid disturbance.

In the case of an *asymmetric* grid disturbance, the amplitudes of the three phase voltages are different, and also the phase separation of 120 degrees is not guaranteed. In the alpha-beta plane asymmetric grid conditions are typically identified by the voltage vector rotating on an ellipse. Figure 2 illustrates such an asymmetric grid condition, which was also measured on the primary side of the transformer at a large gas processing plant in Norway.

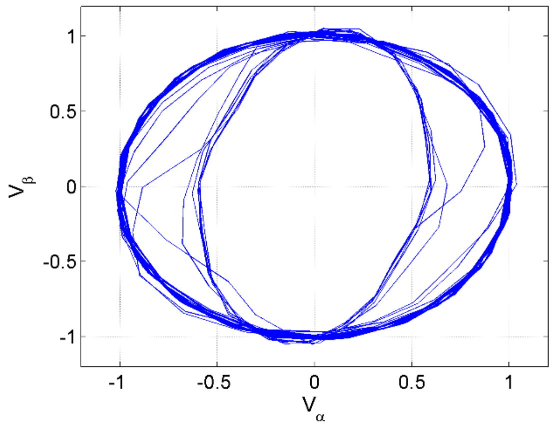

Fig. 2: Example for asymmetric grid disturbance.

B. Ride-Through Characteristics

The reaction of the frequency converter to grid disturbances depends on the physical properties of the frequency converter as well as on the implemented ride-through procedure. As was emphasized in [6], the amount of energy stored in a frequency converter is negligible compared to the transmitted power. The provided power and thus the drive torque is thus dependent on the type and depth of the voltage dip.

We distinguish three classes of ride-through procedures:

1) *Zero-Torque Ride Through:* The operation of the frequency converter is interrupted such that no drive torque is provided by the converter. Operation is resumed when normal grid voltage is available again.

2) *Full-Torque Ride Through:* The frequency converter continues its operation without reduction of the drive torque.

3) *Partial-Torque Ride Through:* The frequency converter continues operation, however only partial torque is provided.

C. Requirements for power loss ride through

The amount of torque necessary to prevent the compressor from going into surge depends on the operating point of the compressor. However, even if the available drive torque is not sufficient to prevent surge, increasing the available drive torque delays the point in time when the compressor enters surge conditions. There is a longer grace period for the grid voltage to recover, and for the initiation of protective measures for the equipment.

The requirements for the ride-through procedure can be summarized as follows:

1. Ensure the frequency converter does not trip e.g. due to overcurrent.
2. Supply either the requested drive torque, or, if that is not possible, as much torque as possible to prevent the compressor from entering surge.
3. Compromise on agreed-upon secondary performance targets in order to increase the drive torque during a ride-through. Examples would be increased torque ripple or a small short-term DC voltage on the VSD transformer.

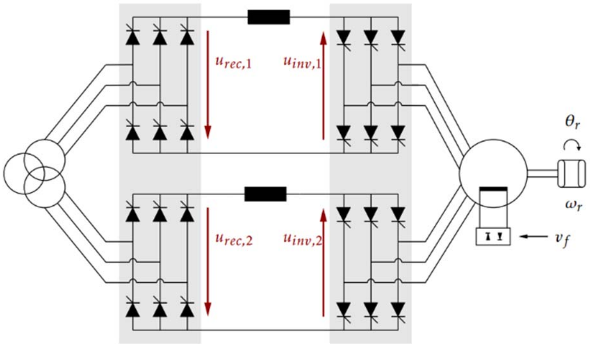

Fig. 3: Variable speed drive system comprised of transformer, load commutated inverter and synchronous machine.

III. SYSTEM DESCRIPTION

The plant processes natural gas from different oil fields in the Northern Sea. It has a capacity of 143,000,000 standard cubic metres (3.8×10^{10} US gal) of natural gas per day. Dry gas is compressed and pumped through four pipe systems to Belgium, France, Germany and the United Kingdom. Six 41.2 MW export compressors are powered by variable speed drive systems comprising dual winding synchronous machines and load commutated inverters.

Fig. 3 depicts a schematic of the employed variable speed drive system comprising a transformer, the load commutated inverter and a synchronous machine. The LCI is in a 2x6/6 pulse configuration with two parallel branches to reduce torque-pulsations. Each branch possesses a six pulse thyristor bridge as line commutated rectifier, a direct current (DC) link and a six pulse thyristor bridge as load commutated inverter. Not shown on this figure are the connection of the drive shaft to the compressor and the connection of the transformer to the medium voltage grid. The transformer employed on site is actually a four-winding three-phase transformer, which is also connected to electric filter banks used for power factor correction and input current harmonic compensation.

The control variables of the variable speed drive system are the firing angles (also called control angles) of the line commutated rectifier and the load commutated inverter, as well as the excitation voltage for the rotor windings. By means of the firing angle of the thyristor bridges, the rectified DC voltages u_{rec} and u_{inv} as well as the direction of power flow can be determined. The machine excitation can be adapted by the excitation voltage v_f.

TABLE 2
DESIGN DATA OF VSD SYSTEM

Parameter	Value	Unit
Line voltage, prim. side	132	kV
Line voltage, sec. side	6200	V
Line frequency	50	Hz
Rated line current, sec. side	2529	A
DC link inductance	7.5	mH
Rated DC current	3342	A
Rated stator voltage	5900	V
Rated stator current	2415	A
Rated stator frequency	60	Hz
Rated shaft power	39.2	MW
Rated rotational speed	3600	rpm

Conventional LCI control schemes assign separate tasks to the control variables: The firing angle β on the machine side are predetermined in order to minimize the reactive power in the machine. The excitation voltage v_f is used to control the stator voltage of the machine. The firing angle α on the line side is actuated to control the current flowing in the DC link, and thus the drive torque. The technical specifications of the variable speed drive system are summarized in Table 2.

IV. PROPOSED CONTROL SOLUTION

In this section the novel model predictive control solution for the LCI is outlined. We start with a generic description of the chosen MPC algorithm, before discussing the application at hand.

A. Generic Description of the MPC Algorithm

Firstly we provide a generic description of the employed model predictive control algorithm [4]. At the heart lies a mathematical model describing the system, and which is used for finite-horizon predictions. This model can be stated as

$$d\mathbf{x}/dt = f(\mathbf{x}(t), \mathbf{u}(t)) \quad (1a)$$
$$\mathbf{y} = g(\mathbf{x}(t), \mathbf{u}(t)) \quad (1b)$$

where:

$\mathbf{u}(t)$	control inputs
$\mathbf{x}(t)$	system states
$\mathbf{y}(t)$	system outputs
f	system equation
g	output equation

Apart from the dynamic model, a cost function is defined which describes the control objectives,

$$J = \int_{kTs}^{kTs+Tp} (\mathbf{x}-\mathbf{x}_{ref})^T \mathbf{Q} (\mathbf{x}-\mathbf{x}_{ref}) + (\mathbf{u}-\mathbf{u}_{ref})^T \mathbf{R} (\mathbf{u}-\mathbf{u}_{ref})\, dt, \quad (2)$$

where reference values are indicated by the subscript ref, k is the sampling instance, Ts the sampling time and Tp the prediction horizon. **Q** and **R** are weight matrices to prioritize the objectives for the MPC controller. Moreover, constraints on the control inputs, states and outputs can be defined:

$$\mathbf{x}\_min \le \mathbf{x} \le \mathbf{x}\_max$$
$$\mathbf{u}\_min \le \mathbf{u} \le \mathbf{u}\_max \quad (3)$$
$$\mathbf{y}\_min \le \mathbf{y} \le \mathbf{y}\_max$$

The continuous-time optimal control problem can thus be stated as

$$\underset{\mathbf{u}}{\text{minimize}}\ (2) \quad \text{subject to}\ (1), (3). \quad (4)$$

The chosen approach to solve the nonlinear problem (4) is a sequential quadratic programming (SQP)-type approach known as real-time iteration scheme with Gauss-Newton approximation of the second-order derivatives. At each time instance a discrete-time linearization of problem (4) is obtained, which corresponds to a quadratic programming (QP) problem. A more detailed description of this solution approach is

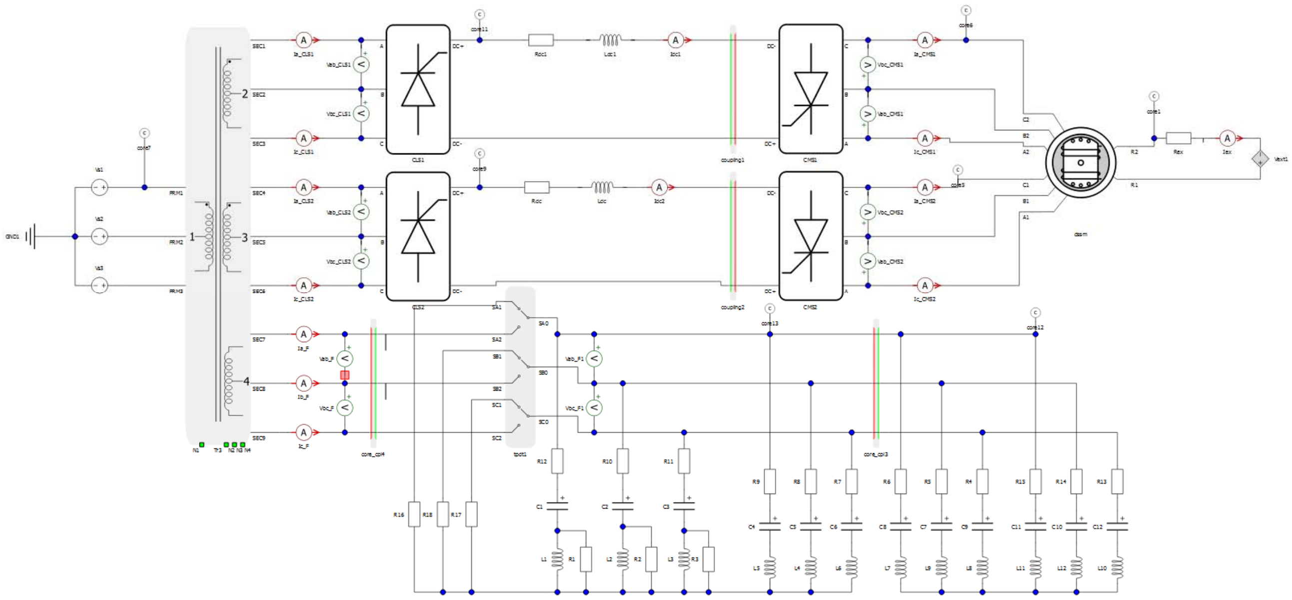

Fig. 4: Schematic of the simulation model on the Hardware-in-the-loop system.

beyond the scope of this paper, and can instead be found in [8]. A highly efficient implementation of this approach is provided by making use of the code generation functionality of the ACADO Toolkit [9]. The resulting QP problem is solved by the on-line QP solver qpOASES [10].

B. Application to Load Commutated Inverters

Some information on the application of the aforementioned MPC algorithm is given in this section. For a more elaborate discussion, see [11], [13], [13].

The model predictive controller is based on a nonlinear dynamic model of the LCI, i.e. of the DC link and the thyristor bridges, which can be stated as

$$\frac{d\,i_{DC}}{dt} = A\, i_{DC} + B_1 \cos\alpha + B_2 \cos\beta, \qquad (5a)$$

$$\tau_e = -\, i_{DC} \cos\beta\,, \qquad (5b)$$

where:

i_{DC}	DC link current
α	Control angle line side (rectifier)
β	Control angle machine side (inverter)
τ_e	Electric torque
A, B	Constants

The control inputs u are the firing angles on the rectifier and on the inverter. The states are the currents in the DC link, and the output is the drive torque of the VSD system. Apart from constraints on the firing angles, an upper bound on the DC link current is defined. Both the control angles of the rectifier and the inverter are selected by the model predictive controller, whereas the excitation voltage control remains independently controlled.

The MPC algorithm was implemented on a control board, which is based on a 32-bit dual-core Power PC processor with a clock cycle of 1.2 GHz. The board also includes a field programmable gate array (FPGA) and a 64-bit floating point unit. The sampling time was chosen to be 1 ms, i.e. at each millisecond a nonlinear mathematical optimization problem is discretized, linearized and solved. Thereby the MPC solution consumes only a minor fraction of the computational resources, such that the whole control system can be executed on time.

Compared to the classical control method, the MPC has the following advantages: (a) Instead of selecting the firing angle on the machine side by means of a predetermined lookup table (i.e. feedforward control), the angle is actively controlled, and can be changed in the case of grid disturbances; (b) instead of executing independent control actions of the firing angles on the line side and the machine side, the MPC coordinates both firing angles to reach the defined objectives; (c) both alternating current (AC) voltage magnitudes are taken into account by the controller; and (d) a constraint on the DC current can be defined to change the control behaviour when the DC current is close to its boundary, thus helping to avoid overcurrent trips.

V. VERIFICATION ON A HIL SYSTEM

Before applying the proposed control solution to a medium voltage drive, its effectiveness was verified on a Hardware-in-the-loop (HIL) system. In this section the findings during this verification are presented.

A. Description of the HIL System

For the verification of the model predictive controller on a HIL system, the control system, consisting of the control hardware and the control software, is exactly as on site. The HIL system is connected via analogue and digital I/Os to the control boards running the control software for the load commutated inverter. The HIL system comprises an FPGA on which a model of the variable speed drive system is simulated in real-time. The dynamics of the drive shaft and the compressor are not included in these simulations, however the compressor behaviour is approximated by a quadratic load torque curve. Another simplification is taken on the grid side. The grid voltages are imposed on the transformer, however the impact of the load commutated inverter on the grid voltage is neglected.

A schematic of the simulation model is depicted in Fig. 4. The upper part contains both branches of the LCI, whereas the lower part shows the electric harmonic filters connected to the transformer.

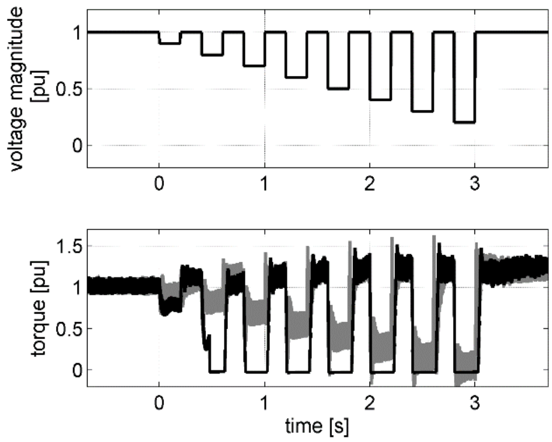

Fig. 5: Simulation results: Grid voltage magnitude and drive torque during symmetric dip series with conventional control (black) and MPC (grey).

B. *Simulations Results*

In this section the simulation results on the HIL system are reported. The behaviour of both the conventional control system and the novel MPC solution are compared during series of symmetric and asymmetric dips.

1) Symmetric Dips: In the first scenario the grid voltage magnitude is decreased in a series of voltage dips with increasing dip depth. Each voltage dip lasts for 200 ms, and the voltage magnitude changes without transition within a microsecond.

Figure 5 depicts the grid voltage magnitude and the electric torque, once with conventional control and once with the novel model predictive controller. No trip occurred regardless of the used controller. However the drive torque provided during the scenario differs significantly. While the conventional control executes a zero-torque ride through procedure for a grid voltage magnitude of 80 % and below, the model predictive controller continues operations and is able to provide partial torque. After the instantaneous reduction of the grid voltage magnitude, the MPC requires about 25 ms to stabilize the drive torque to the steady-state. The amount of residual drive torque decreases with the magnitude of the grid voltage. Full drive torque is guaranteed for a grid voltage magnitude higher than 0.93 pu, i.e. already the step to 0.9 pu voltage magnitude coincides with a reduction of drive torque.

2) *Single-Phase Dips*: The second scenario equals the first one, the difference being that instead of varying the grid voltage magnitude of all phase voltages, only a single phase voltage is changed. That way the controllers are tested under asymmetric grid conditions.

As can be seen in Figure 6, both controllers are able to provide more drive torque if only a single phase is affected. The MPC however outperforms the conventional controller in terms of residual torque.

Based on the conducted simulations, an estimate of the available drive power as a function of the remaining grid voltage can be derived. This estimate is visualized in Fig. 7. As is shown in the Figure, the amount of residual power depends not only on the remaining voltage magnitude, but also on the number of phases which are affected by the grid disturbance. For very low grid voltages operation of the drive is not possible due to problems with estimating the orientation of the grid voltage vector.

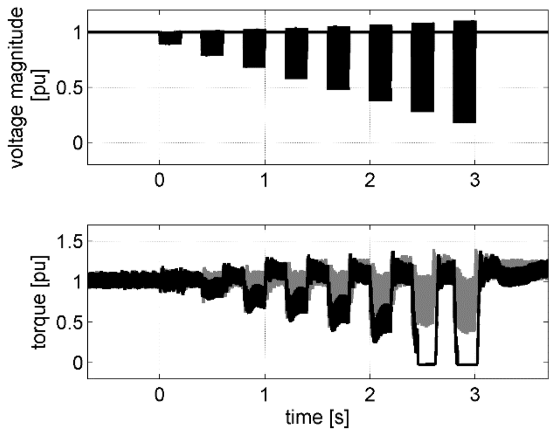

Fig. 6: Simulation results: Grid voltage magnitude and drive torque during single-phase dip series with conventional control (black) and MPC (grey).

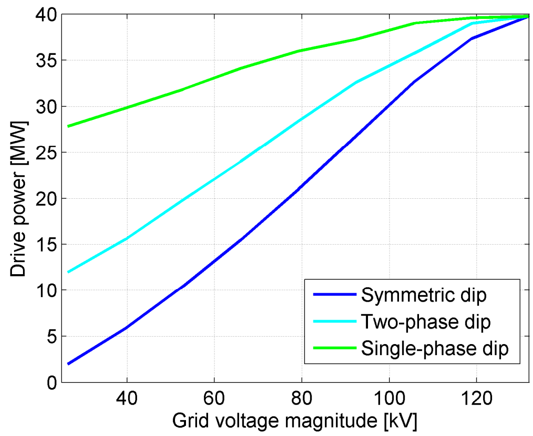

Fig. 7: Estimate of the residual power during voltage dips.

VI. COMMISSIONING ON MV DRIVE

After verifying the effectiveness of the novel control approach on the HIL system, the control system was commissioned on site. Two out of six export compressors on the gas treatment plant were chosen as pilots for the proposed MPC solution. In this section it is shown that under normal grid conditions, the novel control solution works as expected. Fig. 8 shows the speed, the DC current, the control angles and the voltage magnitudes during the first 16 hours of operation. The control behaviour during the commissioning is as expected. The DC link current follows it reference, as provided by the speed controller. A number of speed changes are requested by the process controller, which are delivered swiftly.

A closer look on the start-up of the machine is provided in Fig. 9. Again the behaviour is as expected. First the pulse mode is traversed, then we observe a normal start-up, with switch in of the electric harmonic filters, and reduction of the current reference after the requested speed is reached. The startup procedure is virtually unaffected by the new control system.

Fig. 10 provides an even closer zoom to show the waveforms of the signals under steady-state conditions.

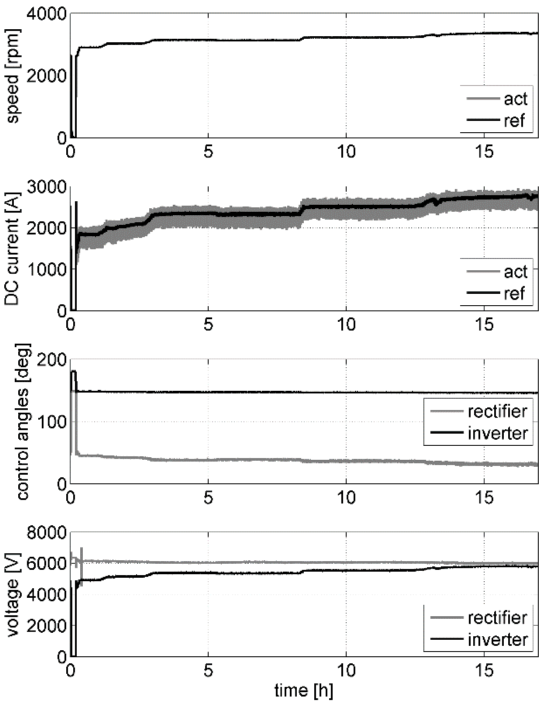

Fig 8: Experimental results: Speed, DC current, control angles and AC voltage magnitudes during the commissioning of the novel control solution.

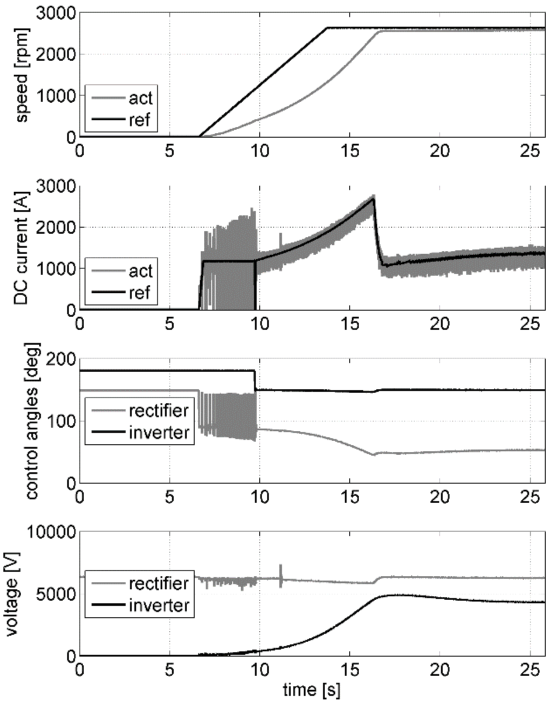

Fig. 9: Experimental results: Zoom to recorded signals at start-up procedure during commissioning.

I. VOLTAGE DIP EVENT

During the course of the winter, a number of grid voltage disturbances occurred. In this section the results of one such case are reported.

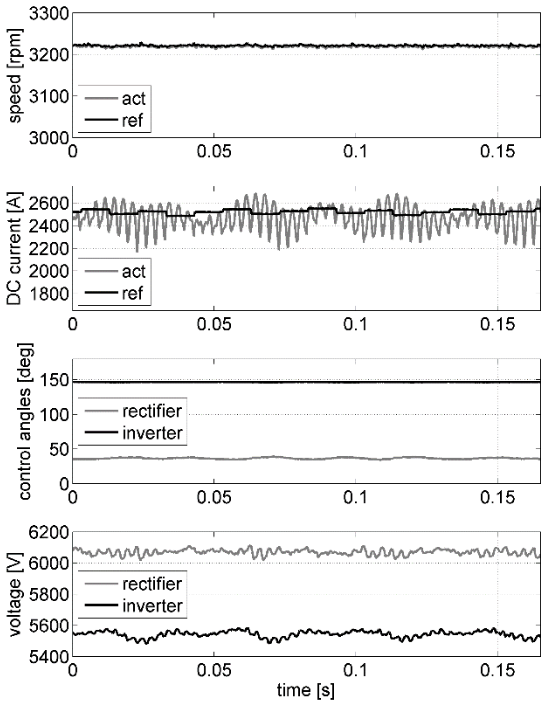

Fig 10: Experimental results: Zoom to waveforms under steady-state conditions.

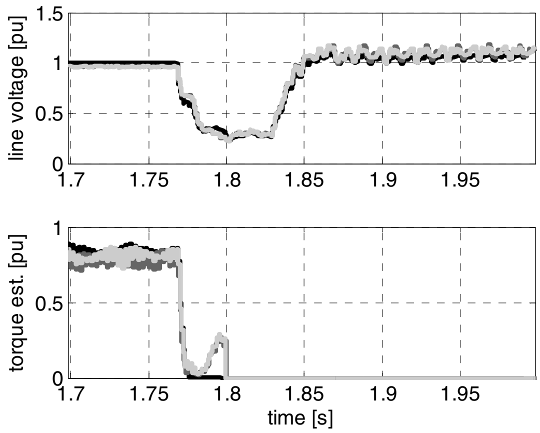

Fig 11: Experimental results: Estimated torque during an undervoltage event. Conventional control (black) vs. MPC solution (dark and light grey).

In Fig. 11 the course of the grid voltage magnitude and an estimate of the drive torque is shown. Since no direct measurement of the drive torque was available, an estimate was calculated from the electric signals of the drive. The black line belongs to an LCI with conventional control, whereas the dark and the light grey lines refer to two LCIs controlled with the new MPC solution.

As can be seen from the plot, the grid voltage is affected by a deep symmetric voltage dip down to about 0.3 pu of the rated grid voltage for a duration of approx. 80 ms. The effect is a significant reduction of the available drive torque. While the conventionally-controlled LCI executes a zero-torque ride through, both MPC-controlled LCIs are subject to an undershoot, from which they recover to provide 0.23 pu of rated drive torque. This result matches the expectations raised by the HIL simulations quite well (0.23 pu torque is a bit more than anticipated). However, the protection system of the gas compressor, which is a timer-based solution not taking into account the available drive torque, trips the operation of the gas compressor approx. 30 ms after the start of the voltage event.

II. CONCLUSION

In this paper the application of a novel model predictive control scheme to load commutated inverters was presented. Simulations on a HIL system have shown its ability to provide partial torque during grid disturbances, and thereby to increase the robustness of electrically-driven gas compression stations.

The control scheme was implemented on two LCIs each powering a 41.2 MW gas compressor on a large gas processing plant in Norway. During voltage dip events in the winter, the ability of the model predictive controlled LCIs to provide partial torque was verified in practice. What remains to be done in order to reap the economic benefits of the solution is a systematic relaxation of the compressor protection system, taking into account the amount of partial torque which is available.

VI. REFERENCES

[1] A. Cortinovis, D. Pareschi, M. Mercangoez, and T. Besselmann, "Model predictive anti-surge control of centrifugal compressors with variable speed drives," *Automatic Control in Offshore Oil and Gas Production, Proceedings of 2012 IFAC Workshop on*, pp 251–256, 2012.

[2] H. Rognø: "Statoil Subsea Factory", Trondheim Gas Technology Conference, June 2014.

[3] E. Wiechmann, P. Aqueveque, R. Burgos, and J. Rodriguez, "On the Efficiency of Voltage Source and Current Source Inverters for High Power Drives," *Industrial Electronics, IEEE Transactions on*, vol. 55, pp. 1771–1782, April 2008.

[4] J. Rawlings and D. Mayne, *Model Predictive Control: Theory and Design*. Nob Hill Pub., 2009.

[5] H. Peyrl, A. Zanarini, T. Besselmann, J. Liu, and M.-A. Boéchat, "Parallel implementations of the fast gradient method for high-speed MPC," *Control Engineering Practice*, vol. 33, no. 0, pp. 22–34, 2014.

[6] T. Wymann and P. Jörg, "Power loss ride-through in a variable speed drive system," *PCIC Europe Conference Record*, Amsterdam, Netherlands, pp 1–9, June 2014.

[7] W. C. Duesterhoeft, M.W. Schulz and E. Clarke, "Determination of Instantaneous Currents and Voltages by Means of Alpha, Beta, and Zero Components". *Transactions of the American Institute of Electrical Engineers,* vol 70 (2), pp 1248–1255, July 1951.

[8] M. Diehl, H. Bock, J. Schlöder, R. Findeisen, Z. Nagy, and F. Allgöwer, "Real-time optimization and Nonlinear Model Predictive Control of Processes governed by differential-algebraic equations," *Process Control, Journal on*, vol. 12, no. 4, pp. 577–585, 2002.

[9] B. Houska, H. Ferreau, and M. Diehl, "An Auto-Generated Real-Time Iteration Algorithm for Nonlinear MPC in the Microsecond Range," *Automatica*, vol. 47, no. 10, pp. 2279–2285, 2011.

[10] H. Ferreau, C. Kirches, A. Potschka, H. Bock, and M. Diehl, "qpOASES: A parametric active-set algorithm for quadratic programming," *Mathematical Programming Computation*, vol. 6, no. 4, pp. 327–363, 2014.

[11] T. Besselmann, S. Van de moortel, S. Almér, P. Jörg and H.J. Ferreau, "Model Predictive Control in the Multi-Megawatt Range", *IEEE Transactions on Industrial Electronics*, vol. 63, no. 7, pp. 4641-4648, July 2016.

[12] T. Besselmann, S. Almér, H.J. Ferreau, „Model Predictive Control of Load Commutated Inverter-fed Synchronous Machines", *IEEE Transactions on Power Electronics*, vol. 31, no. 10, pp. 7384-7393, Oct. 2016.

[13] S. Almér, T. Besselmann, and J. Ferreau, "Non-linear model predictive torque control of a load commutated inverter and synchronous machine", *International Power Electronics Conference, ECCE-ASIA*, Hiroshima, Japan, pp 3563–3567, May 2014.

VIII. VITA

Thomas Besselmann graduated from the Hamburg University of Technology in 2005 with a Dipl.-Ing. degree in mechatronics. In 2010 he received his Ph.D. degree at the Automatic Control Laboratory, ETH Zurich. Currently he is employed as senior scientist in the Control & Optimization group at ABB Corporate Research.
thomas.besselmann@ch.abb.com

Pieder Jörg received his M.Sc. degree 1995 from the Swiss Federal Institute of Technology, Zurich. He joined ABB at Corporate Research in the area of power electronics. In 2002 he joined the business unit Medium Voltage Drives as head of product development. Since 2010 he is focusing on business and technology development for demanding drives applications. He has been involved in various studies and improvement projects involving large VSD systems with demanding rotor dynamics.
pieder.joerg@ch.abb.com

Terje Knutsen received his M.Sc. degree in Electrical engineering from the Norwegian University of Technology and Science (former NTH) in Trondheim in 1985. He has held various positions within Siemens in Norway and Germany with main topic Variable Speed Drives Systems before he joined Statoil January 2013 and is currently working as a Principal Engineer in Facilities Technology.
tekn@statoil.com

Erling Lunde received his PhD in Engineering Cybernetics, Robot control theory, from the Norwegian University of Technology and Science (former NTH) in Trondheim in 1991. Since then he worked as a consultant in cybernetics for a large number of industrial clients within marine automation, process control, hydraulics, and more. He was employed by Statoil in 2012 and is currently working as a Principal Researcher in Facilities Technology.
elunde@statoil.com

Tor Olav Stava graduated from the Stord/Haugesund University College in 2009 with a bachelor degree in process and energy technology. Currently he is employed

as a senior engineer in the Technology department in Gassco.
toros@gassco.no

Sture Van de moortel graduated from the University of Applied Science in Lucerne in 2006 with a Dipl.-Ing. degree in electrical engineering. In 2007, he started his professional career at ABB Medium Voltage Drives and held different positions over the past years. His focus has been LCI control and application software until he recently joined a Drive System Expert team focusing on large VSD systems, rotor dynamics, advanced regulation and interdisciplinary collaboration with our partners from industry.
sture.vandemoortel@ch.abb.com